QG Barotropic Vorticity Equation

The goal of this investigation was to solve the following quasi-geostrophic (QG) barotrophic vorticity equation:

$$\frac{\partial \varsigma}{\partial t} = -J(\psi, \varsigma) - \beta \frac{\partial \psi}{\partial x} \tag{1}$$

$$\frac{\partial^2 \psi}{\partial x^2} + \frac{\partial^2 \psi}{\partial y^2} = \zeta(x, y) \tag{2}$$

In this method, the advection term was defined used Arakawa discretization of the 2D Jacobian. This discrete equation conserves kinetic energy, enstrophy, and prevents the build up of energy at small scales. The discretization scheme involves three methods of calculating the Jacobian, outlined in equations (3), (4) and (5). The Arakawa discretization then uses the average of the three to advect the solution (equation (6)).

$$J(\psi, \varsigma) \cong \frac{1}{2\Delta x}\left(\psi_{i+1,j} - \psi_{i-1,j}\right)\frac{1}{2\Delta y}\left(\varsigma_{i,j+1} - \varsigma_{i,j-1}\right) - \frac{1}{2\Delta y}\left(\psi_{i,j+1} - \psi_{i,j-1}\right)\frac{1}{2\Delta x}\left(\varsigma_{i+1,j} - \varsigma_{i-1,j}\right) \tag{3}$$

$$\begin{aligned}\hat{J}(\psi, \varsigma) \cong\ & \frac{1}{2\Delta x}\left(\psi_{i+1,j}\frac{1}{2\Delta y}\left(\varsigma_{i+1,j+1} - \varsigma_{i+1,j-1}\right) - \psi_{i-1,j}\frac{1}{2\Delta y}\left(\varsigma_{i-1,j+1} - \varsigma_{i-1,j-1}\right)\right) \\ & - \frac{1}{2\Delta y}\left(\psi_{i,j+1}\frac{1}{2\Delta x}\left(\varsigma_{i+1,j+1} - \varsigma_{i-1,j+1}\right) - \psi_{i,j-1}\frac{1}{2\Delta x}\left(\varsigma_{i+1,j-1} - \varsigma_{i-1,j-1}\right)\right)\end{aligned} \tag{4}$$

$$\begin{aligned}\tilde{J}(\psi, \varsigma) \cong\ & \frac{1}{2\Delta y}\left(\varsigma_{i,j+1}\frac{1}{2\Delta x}\left(\psi_{i+1,j+1} - \psi_{i-1,j+1}\right) - \varsigma_{i,j-1}\frac{1}{2\Delta x}\left(\psi_{i+1,j-1} - \psi_{i-1,j-1}\right)\right) \\ & - \frac{1}{2\Delta x}\left(\varsigma_{i+1,j}\frac{1}{2\Delta y}\left(\psi_{i+1,j+1} - \psi_{i+1,j-1}\right) - \varsigma_{i-1,j}\frac{1}{2\Delta y}\left(\psi_{i-1,j+1} - \psi_{i-1,j-1}\right)\right)\end{aligned} \tag{5}$$

$$J(\psi, \varsigma) \equiv \frac{1}{3}(J + \hat{J} + \tilde{J}) \tag{6}$$

A detailed explanation of how the Poisson equation (2) was solved can be found in the report for Modeling Task #5. The same method of SOR iterating was employed in this task as well. For each time evolution, stream function was set to 0 throughout the domain in order to force a recalculation of all the points.

In order to step in time, Euler-Forward (EF) was used in the first two time-steps. Successive time-steps were calculated using AB3. The recursive equations for EF (7) and AB3 (8) are as follows:

$$\varsigma_{i,j}^{n+1} = \varsigma_{i,j}^{n} - [J(\psi, \varsigma)]_{i,j}^{n}\Delta t - \beta\left(\frac{\psi_{i+1,j}^{n} - \psi_{i-1,j}^{n}}{2\Delta x}\right) \tag{7}$$

$$\begin{aligned}\varsigma_{i,j}^{n+1} =\ & \frac{23}{12}\left(-\left[J(\psi, \varsigma)\right]_{i,j}^{n}\Delta t - \beta\left(\frac{\psi_{i+1,j}^{n} - \psi_{i-1,j}^{n}}{2\Delta x}\right)\right) \\ & - \frac{16}{12}\left(-\left[J(\psi, \varsigma)\right]_{i,j}^{n-1}\Delta t - \beta\left(\frac{\psi_{i+1,j}^{n-1} - \psi_{i-1,j}^{n-1}}{2\Delta x}\right)\right) \\ & + \frac{5}{12}\left(-\left[J(\psi, \varsigma)\right]_{i,j}^{n-2}\Delta t - \beta\left(\frac{\psi_{i+1,j}^{n-2} - \psi_{i-1,j}^{n-2}}{2\Delta x}\right)\right) + \varsigma_{i,j}^{n}\end{aligned} \tag{8}$$

To test this method, four simulations were tested. Experiment #1, the “original” case, had no coriolis effect acting on the domain, the radius of each vortex was a = 180 km, they were separated by a distance of b = 600 km, and there were both rotating in the same direction (counter-clockwise).

Experiment #2, the “coriolis” case, simulated the effect of coriolis with $\beta = 2 \times 10^{-8}$ /km /s. The other parameters were the same as in Experiment #1.

Experiment #3, the “dipole” case, was the same as Experiment #1 except the vortices were rotating in opposite directions. In particular, the right vortex was rotating clockwise.

Experiment #4, the “ratio” case, used a = 100 km with other parameters as outlined in Experiment #1.

Due to lack of time, the results for Experiment #1 are shown below. The findings from Experiments #2 - #4 as briefly discussed afterwards.

A time-step of $\Delta t = 500$ seconds was used to evolve the solution as, with this, we had Courant’s number proportional to 500 s / 20 km. As is discussed lated, this means that Courant number was in the range of 0.2 to 0.24 which is well in the stable range for AB3 and EF as well.

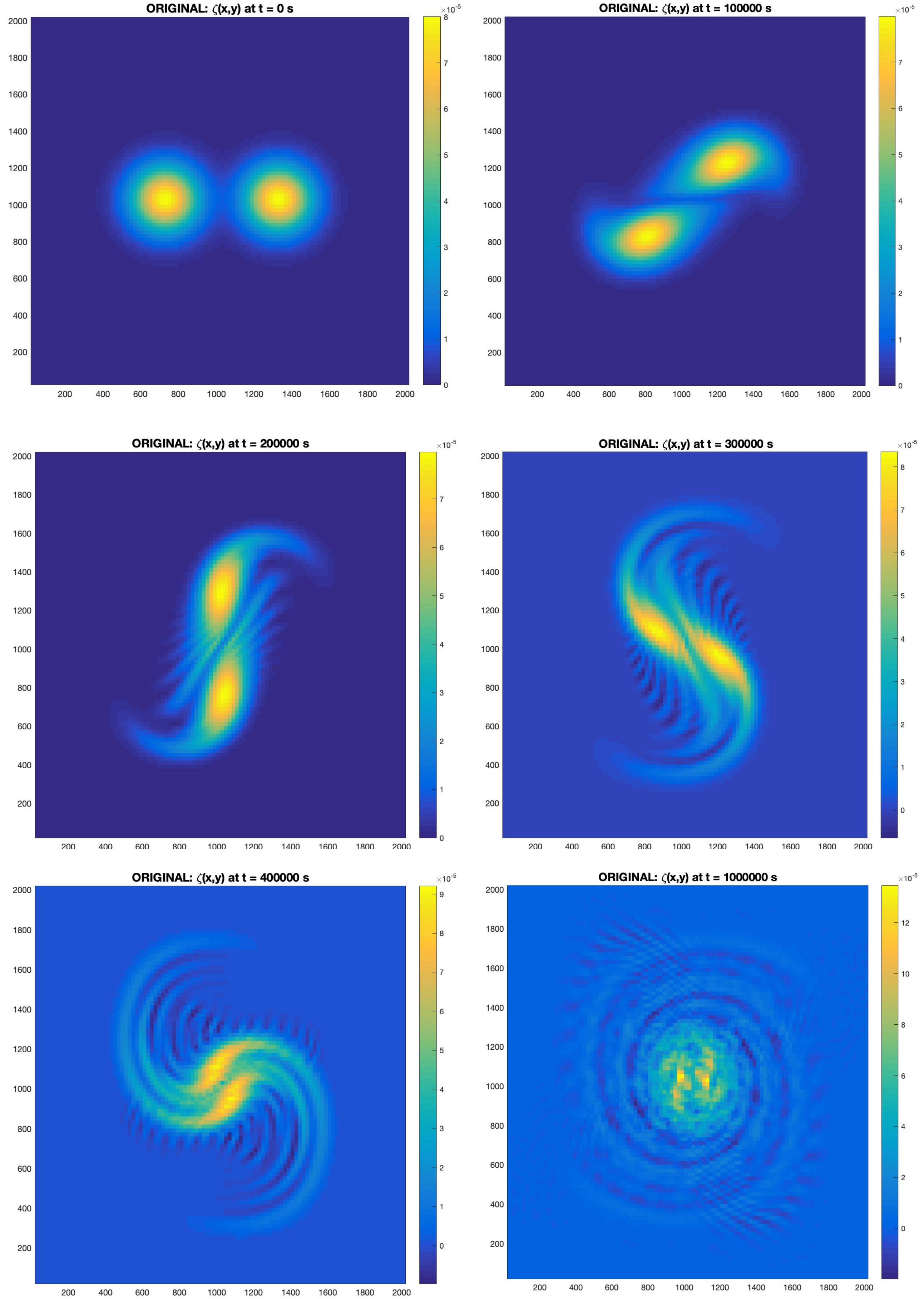

Figure 1 shows the evolution of the vortices at the stated times. As can be seen, with an a : b ratio of 180 :

600, the two vortices merge quite well. We see that AB3 is a good in evolving the solution. However, AB3 does have one physical mode and two computations modes as its stability analysis results in a third order equation for the amplification factor. While it is difficult to see the physical mode and amplification, the computational mode can be spotted by the irregularity of the ripples that are formed in the vortices wake by the time t = 1,000,000 s.

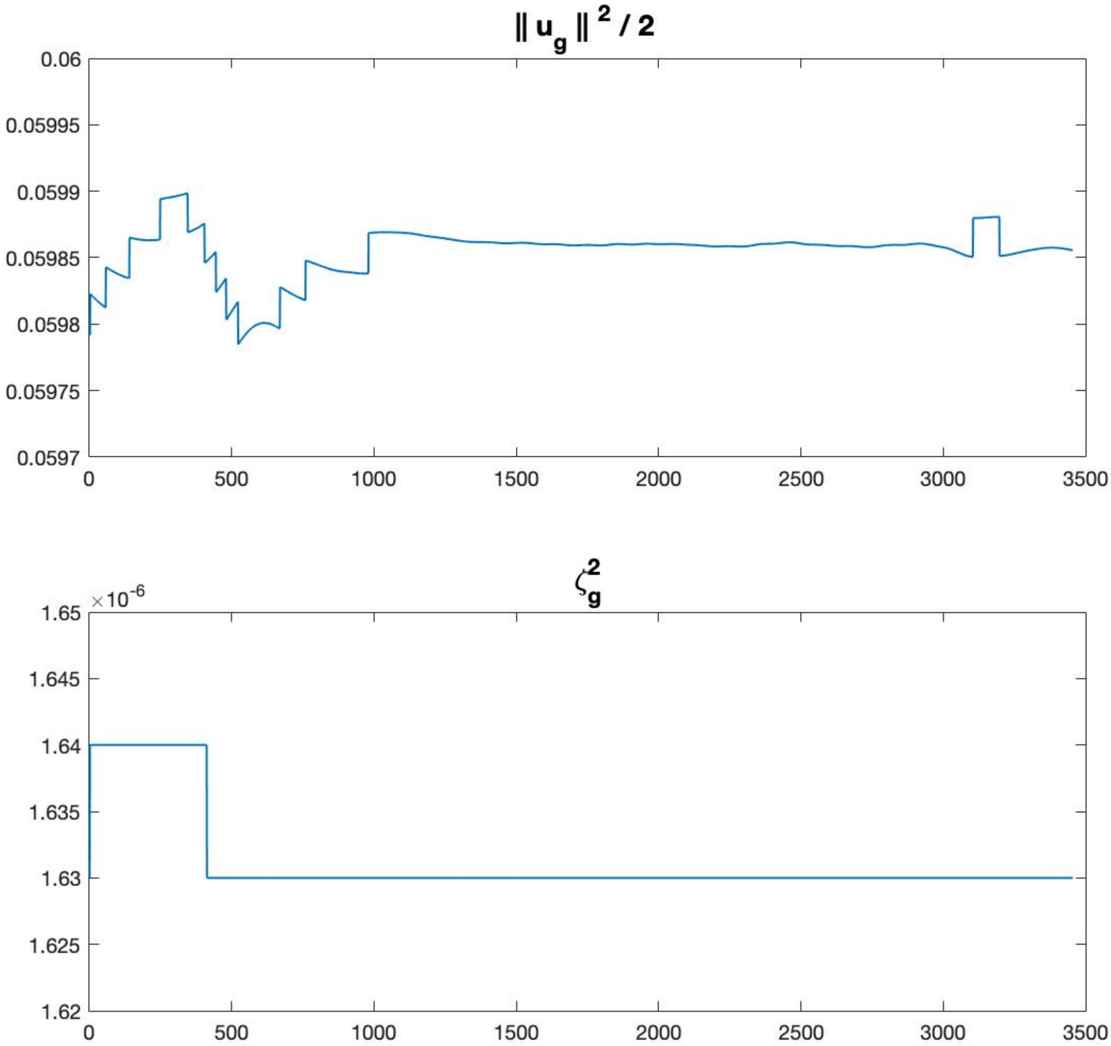

Figure 2 shows the plots of kinetic energy and enstrophy over the domain for every time evolution of the solution. As we can see, there are small deviations in kinetic energy initially. These are one the other of 10^{-3}. The plot has step-like features, suggesting that such deviations are most likely due to truncation errors. After 1000 iterations, kinetic energy is more or less stable throughout the simulation. Enstrophy has an initial jump and then returns to the initial value before 500 iterations are completed. As the order of this change is even smaller, it can be treated as almost negligible. As kinetic energy and enstrophy were to be conserved in this simulation, we can say that while it was not satisfied with great accuracy, the method used is still stable.

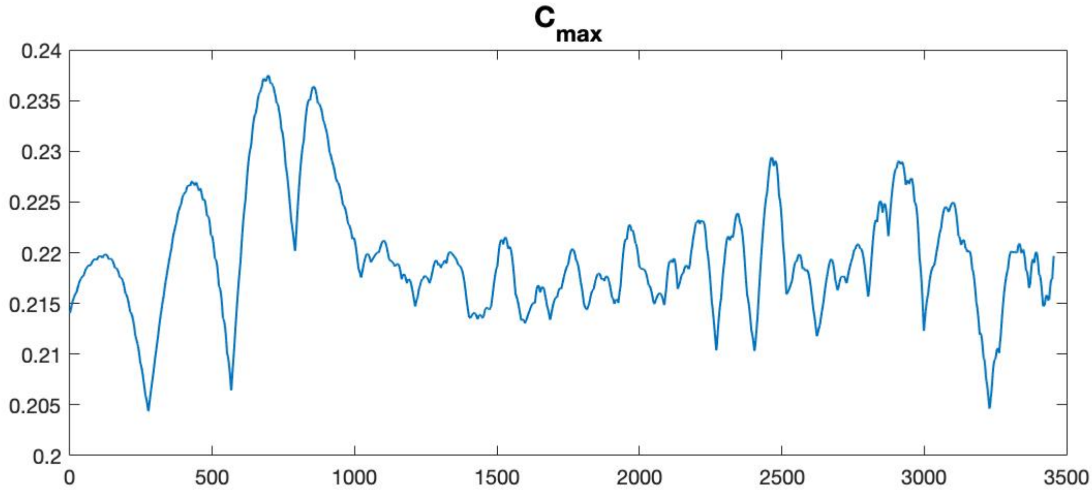

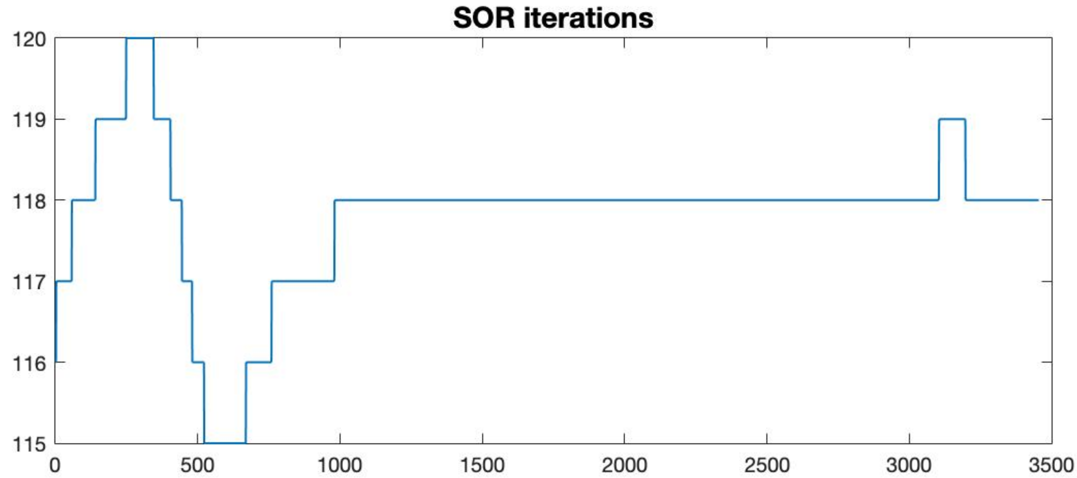

Figure 3 shows the maximum Courant number over the domain and the number of SOR iterations required in the Poisson solver. As we can see, Courant number stays in the range of 0.2 to 0.24 throughout the simulation with the greatest fluctuations occurring initially. This further supports the conclusion that the method used is stable. The stream function was reset to 0 across the domain for every time-step in order to force computation. As we can see, it consistently took between 115 and 120 iterations to solve the Poisson equation. After 1000 iterations, the number of iterations remained relatively constant at 118 for each time step. This corresponds to when kinetic energy fluctuations were no longer observed.

Experiment #2 explored the effect of coriolis on the domain. For the value of β chosen, the difference in the evolution of the vortices was not particularly different. In Experiment #1, by the end of the 20 day period of observation, the vortex centers were no longer distinguishable whereas in Experiment #2, they were still distinguishable. The ripples were also more regular whereas in Experiment #1, the wake of the vortices were merged and become a little ‘messy’ overall. When beta was increased in magnitude, an overall clockwise advection of the merging vortices was observed. This resulted in the vortices merging off-center in the domain.

Experiment #3 saw no merging of vortices. The one on the left rotated counterclockwise while following a convective cell trajectory on the left half of the domain. The vortex on the right rotated clockwise and advected on the right. During the period of evolution of 20 days, their speeds and positions mirrored each other and stayed consistent. With further iterations, the interactions of computational modes from each vortex on the other became increasingly clear. At times, the shapes of vortices were skewed and elongated.

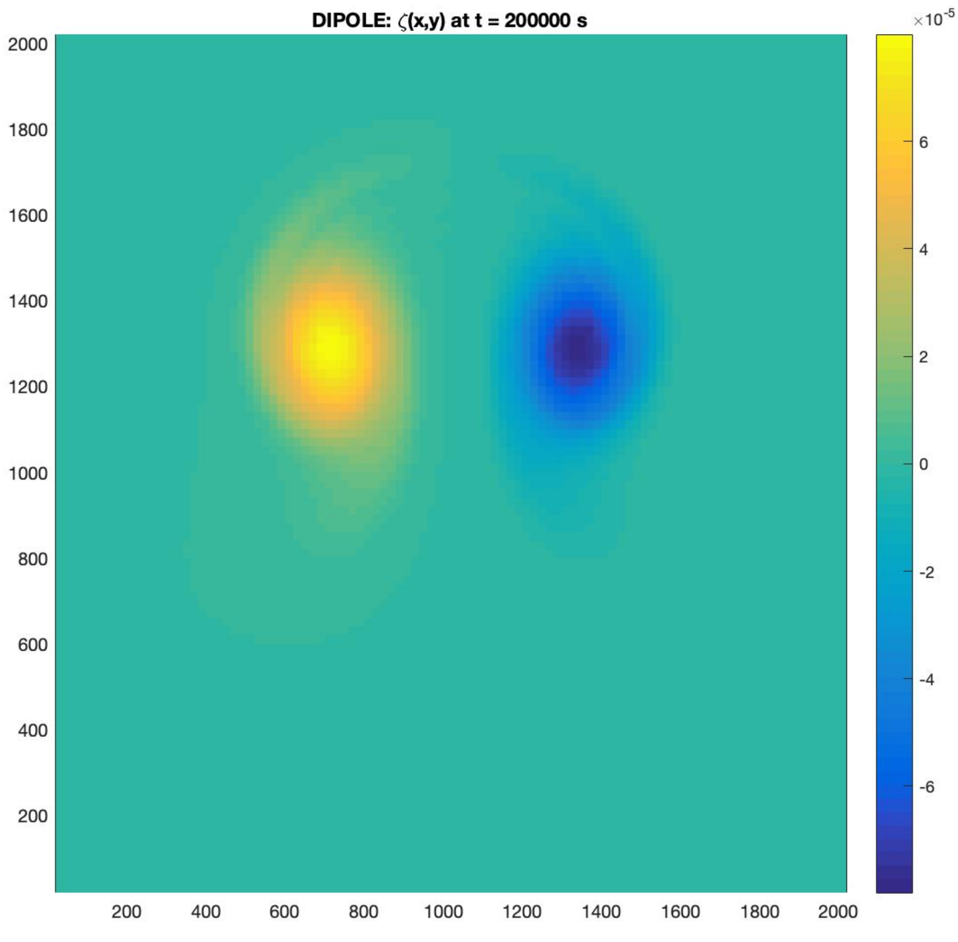

Experiment #4 also saw no merging of vortices. For the entire duration of observation, the vortices continued to rotate around each other but did not get closer. We see the evolution of computational modes as the simulation evolves in time.